

A quantum chemical guided interpretation of the infrared and Raman spectra of trimethylsilyl trifluoromethanesulfonate, $\text{CF}_3\text{SO}_2\text{OSi}(\text{CH}_3)_3$

L.E. Fernandez^a, A. Ben Altabef^{a,1}, E.L. Varetti^{b,1,*}

^aInstituto de Química y Física, Facultad de Bioquímica, Química y Farmacia, Universidad Nacional de Tucumán, San Lorenzo 456, 4000 San Miguel de Tucumán, Argentina

^bCEQUINOR (Centro de Química Inorgánica, CONICET, UNLP), Departamento de Química, Facultad de Ciencias Exactas, Universidad Nacional de La Plata, C.Correo 962, 1900 La Plata, Argentina

Received 9 July 1999; accepted 24 April 2000

Abstract

The optimized structure and the wavenumbers of the normal modes of vibration were calculated for $\text{CF}_3\text{SO}_2\text{OSi}(\text{CH}_3)_3$ using density functional theory (DFT) methods, with a B3LYP functional and the 6-31G** basis set. The calculations predict a *gauche* conformation of the $\text{Si}(\text{CH}_3)_3$ group with respect to the rest of the molecule, in agreement with the conformations found experimentally and theoretically for related molecules. The infrared spectra of the gas and liquid phases as well as the Raman spectrum of the liquid substance were obtained and interpreted on the basis of the calculated spectrum and the published data for related substances. © 2000 Elsevier Science B.V. All rights reserved.

Keywords: Trimethylsilyl; Trifluoromethanesulfonate; DFT calculations; Infrared; Raman

1. Introduction

Trimethylsilyl trifluoromethanesulfonate, $\text{CF}_3\text{SO}_2\text{O-Si}(\text{CH}_3)_3$, is a commercially available substance widely used in silylating and other organic reactions. As neither the molecular structure nor the vibrational characteristics of this substance were reported, we decided to extend to it our previous study on silyl trifluoromethanesulfonate, $\text{CF}_3\text{SO}_2\text{OSiH}_3$ [1]. For that purpose, the infrared and Raman spectra were measured and an opti-

mized molecular structure and wavenumbers corresponding to the normal modes of vibration were calculated by means of quantum chemical procedures. The spectral features were subsequently assigned to the different normal modes of vibration.

2. Experimental part

The substance is a commercial product (Aldrich, 99% nominal) and was used with no further purification. It was handled with proper protection from the atmospheric humidity.

The infrared spectra were run in Bruker FTIR instruments, models IFS 66 and IFS 113v. The FRA 106 accessory was used in the former instrument to

* Corresponding author. Tel.: +54-221-4259485; fax: +54-221-4240172.

E-mail address: varetti@dalton.quimica.unlp.edu.ar (E.L. Varetti).

¹ Members of the Carrera del Investigador Científico, CONICET (Argentina).

Table 1

Geometrical parameters calculated for $\text{CF}_3\text{SO}_2\text{OSi}(\text{CH}_3)_3$. Atom numbers appear in Fig. 1

Bond lengths (Å)		Bond angles (°)		Dihedral angles (°)	
C2–F1	1.332	F1–C2–F3	109.4	C2–S5–O7–Si8	113.1
C2–F3	1.337	F3–C2–F4	109.3	F1–C2–S5–O7	178.3
C2–F4	1.331	F1–C2–F4	109.7	S5–O7–Si8–C9	179.5
C2–S5	1.868	F1–C2–S5	108.6	Si8–O7–S5–O21	1.3
S5–O6	1.452	O6–S5–O21	121.6	O7–Si8–C9–H10	179.7
S5–O21	1.461	C2–S5–O6	107.0	O7–Si8–C13–H14	176.4
S5–O7	1.591	C2–S5–O21	107.0	O7–Si8–C17–H18	177.2
O7–Si8	1.759	C2–S5–O7	98.4		
Si8–C9	1.872	C7–S5–O21	110.6		
Si8–C13	1.872	C7–S5–O6	109.5		
Si8–C17	1.873	S5–O7–Si8	128.9		
C9–H10	1.096	O7–Si8–C17	108.6		
C9–H11	1.094	C9–Si8–C17	112.9		
C9–H12	1.094	C9–Si8–C13	113.2		
C13–H14	1.096	C13–Si8–C17	112.7		
C13–H15	1.095	Hi–C9–Hj	107.9 ^a		
C13–H16	1.094	Hi–C13–Hj	108.0 ^a		
C17–H18	1.096	Hi–C17–Hj	108.1 ^a		
C17–H19	1.093	Si8–C9–H10,11,12	111.0 ^a		
C17–H20	1.094	Si8–C13–H14,15,16	110.9 ^a		
		Si8–C17–H18,19,20	110.8 ^a		

^a Mean values.

obtain the Raman spectrum of the substance, using light of 1.064 μm from a Nd/YAG laser for excitation.

A glass cell of 19.5 cm optical path provided with Si windows was used to obtain the spectra of the gaseous substance. The Raman spectrum was obtained with the liquid contained in the original ampoule or in a 5 mm ID glass tube.

The gas phase infrared spectra showed a band located at 1073 cm^{-1} whose relative intensity changed in different experiments. It was therefore considered as due to an impurity, probably resulting from the reaction of the substance with traces of atmospheric water in the cell. This band did not appear in the infrared or the Raman spectra of the liquid substance.

3. Calculations

The molecular geometry was optimized by means of density functional theory (DFT) methods, with a B3LYP functional [2,3] and the 6-31G** basis set, as provided with the GAUSSIAN94 suit of programs [4]. The wavenumbers corresponding to the normal modes

of vibration were subsequently calculated with the same approximation. Besides, the potential energy surface was explored using the RHF technique and the same basis set, in order to detect secondary minima.

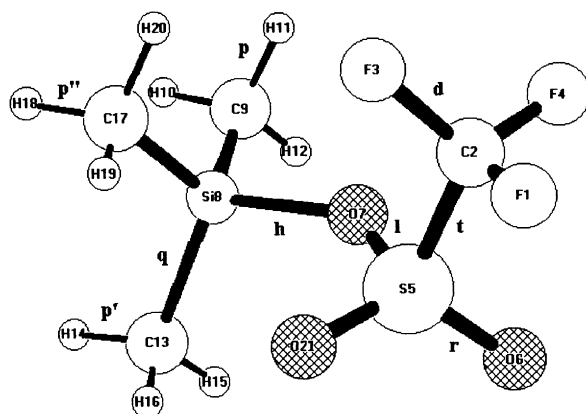
The harmonic force field in Cartesian coordinates which resulted from the DFT procedure was transformed to local symmetry coordinates through the corresponding *B* matrix [5], calculated with a standard program, and the potential energy distribution was subsequently obtained; those calculations were performed with the program FCARTP [6].

The program HYPERCHEM [7] was used to represent graphically the atomic displacements given by the GAUSSIAN programs for each vibrational mode, allowing a qualitative understanding of the nature of some vibrations.

4. Results and discussion

4.1. Structure

A selection of geometrical parameters resulting



Definition of angles:

π : H - C - H	μ : C - Si - O	γ : O7 - S - O6,21
ϕ : Si - C - H	α : Si - O - S	τ CH ₃ : O - Si - C _i - H _j
ϵ : F - C - F	ϕ : O = S = O	τ S-O : C - S - O - Si
β : S - C - F	θ : C - S - O7	τ CF ₃ : O - S - C - F _i
λ : C - Si - C	ψ : C - S - O6,21	τ SiC ₃ : S - O - Si - C _i

Fig. 1. The calculated molecular structure, atom numbering and definition of internal coordinates for $\text{CF}_3\text{SO}_2\text{OSi}(\text{CH}_3)_3$.

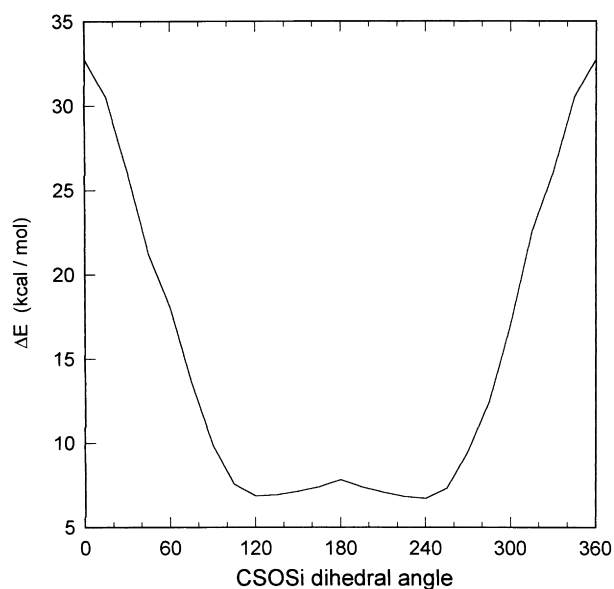


Fig. 2. Relative energy of the $\text{CF}_3\text{SO}_2\text{OSi}(\text{CH}_3)_3$ molecule as a function of the CSOSi dihedral angle (0° correspond to eclipsed C_2 and SiO).

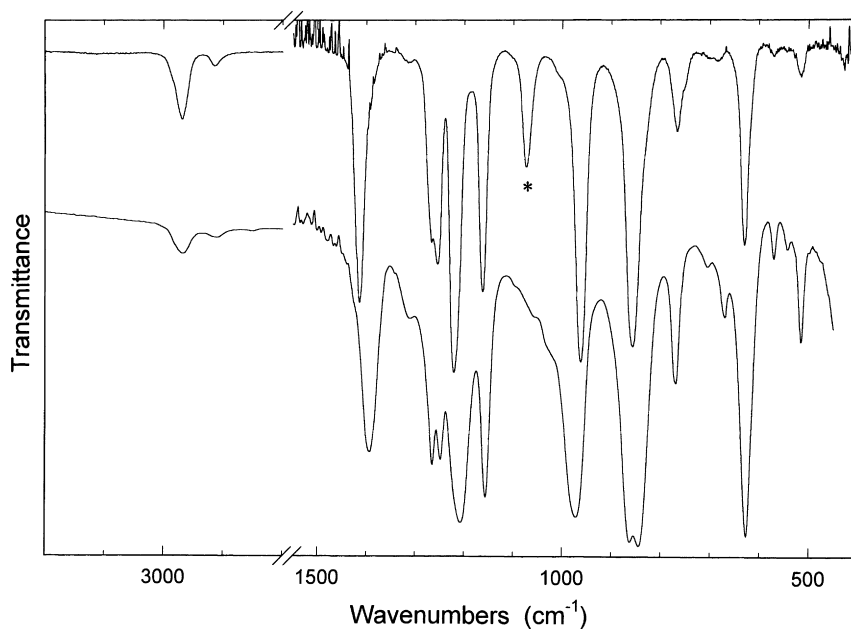


Fig. 3. Mid-infrared spectra of $\text{CF}_3\text{SO}_2\text{OSi}(\text{CH}_3)_3$. Upper: gas phase; path length: 19.5 cm; pressure: ca. 0.3 mbar; resolution: 1 cm^{-1} ; impurity band marked with asterisk (see text). Lower: liquid phase; film between AgCl windows; resolution: 4 cm^{-1} .

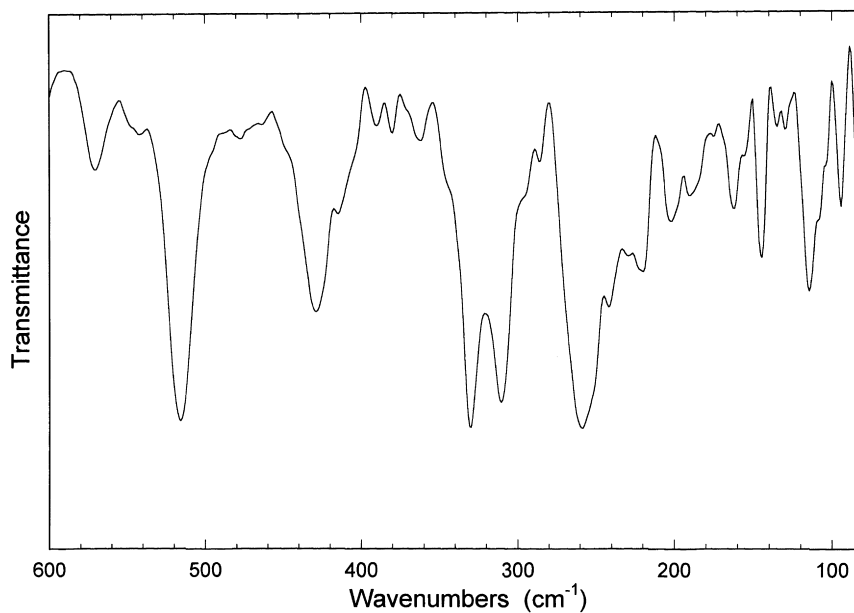


Fig. 4. Far-infrared spectrum of $\text{CF}_3\text{SO}_2\text{OSi}(\text{CH}_3)_3$. Path length: 19.5 cm; vapor in equilibrium with liquid; resolution: 4 cm^{-1} .

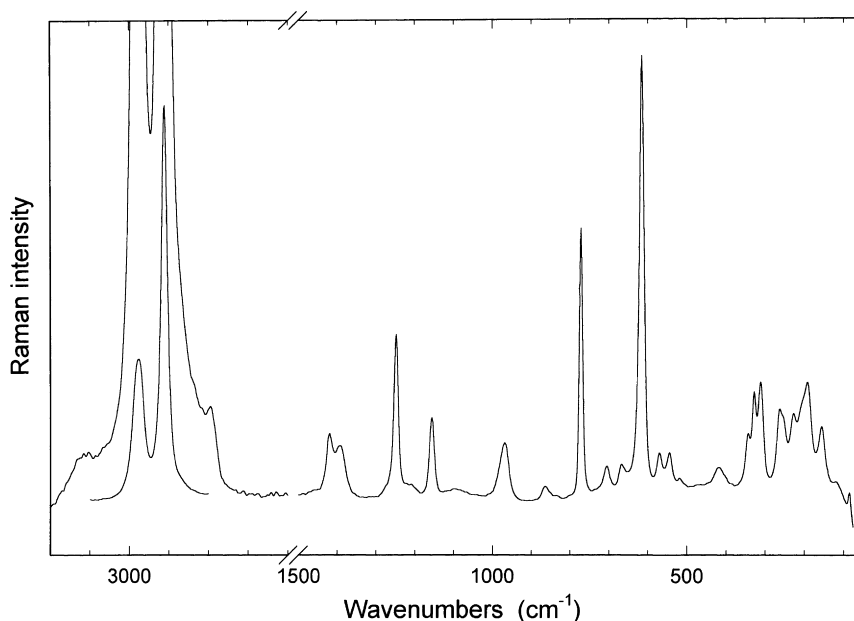


Fig. 5. Raman spectrum of $\text{CF}_3\text{SO}_2\text{OSi}(\text{CH}_3)_3$ at 4 cm^{-1} resolution. The intensity (height) ratio between the 2912 and the 616 cm^{-1} bands is 7.2.

from the optimization procedure appears in Table 1. Such parameters are very similar to those calculated for the silyl compound [1], as expected.

Particularly interesting is the resulting CSOSi dihedral angle, which gives the molecule a *gauche* conformation (Fig. 1), having an energy $E = -1370.7432314$ Hartree. In fact, this is also the conformation found experimentally and theoretically for methyl trifluoromethanesulfonate and other sulfonates [8]. Such dihedral angles in the trimethylsilyl- and in the silyl-trifluoromethanesulfonates have the highest values calculated as yet: 113.1° and 110.3° , respectively.

A search for secondary minima in the potential energy surface was performed by means of a series of calculations in which the molecular geometry was optimized for fixed values of the C2S5O7Si8 dihedral angle, in 15° steps. Due to computational limitations, the HF/6-31G** approximation was used in such calculations and only three parameters were allowed to change: the S5O7Si8C9 (SiC₃ torsion) and F3C2S5O7 (CF₃ torsion) dihedral angles and the C2S5O7 angle. The results of such calculations are shown in Fig. 2 as differences with respect to the molecular energy resulting from a full optimization with the

same theoretical approximation ($E = -1366.0635514$ Hartree, CSOSi = 121.4°). It can be seen that only two equivalent and symmetrically located minima exist, at ca. 120° and 240° , separated by a very shallow barrier amounting to 1.12 kcal/mol, which suggests a rapid interchange between both equilibrium minima. The 113.1° value mentioned above for the CSOSi dihedral angle should approach more closely the real position of the minimum located at ca. 120° .

A consideration of the calculated dihedral angles for this molecule (Table 1) reveals two interesting conformational characteristics. The first one is that the methyl groups are symmetrically arranged so as to minimize their mutual repulsion, with one CH bond per methyl group quasi-parallel to the SiO bond. The second one is the eclipsed orientation of the SiO bond relative to the S5=O21 double bond, being the SiC9 bond practically in the same plane as the other two.

4.2. Vibrational spectra

Representative infrared and Raman spectra for the studied molecule appear in Figs. 3–5, whereas the wavenumbers of the observed spectral features are collected in Table 2. The wavenumbers calculated

Table 2

Observed bands in the infrared and Raman spectra of $\text{CF}_3\text{SO}_2\text{OSi}(\text{CH}_3)_3$ (s: strong; m: medium; w: weak; v: very; sh: shoulder; br: broad)

Infrared (gas)	Infrared (liq.)	Raman (liq.) ^a	Assigned to
2970 m	2968	2977 ^a	$\nu_1-\nu_6$
2915 w	2912	2912 ^a	$\nu_7-\nu_9$
1420 sh	1427 sh	1420 (14)	$\nu_{10}-\nu_{15}$
1414 s	1394	1393 (11)	ν_{16}
1311 w	1313	—	$705 + 616 = 1321$
1264 sh	1264	1275 sh, vw	$\nu_{17}-\nu_{20}$
1255 s	1247	1249 (36)	$\nu_{17}-\nu_{20}$
1221 vs	1207	1208 vvw	ν_{21}, ν_{22}
1163 s	1156	1156 (18)	ν_{23}
962 vs	971	968 br (13)	ν_{24}
857 vs	860	865 (4)	ν_{25}, ν_{26}
—	842	849 sh, vvw	ν_{27}
767 m	768	772 (62)	$\nu_{28}-\nu_{30}$
ca. 700 sh	705	706 (5)	$\nu_{31}-\nu_{33}$
683 w	670	668 (3)	ν_{34}
630 s	626	—	ν_{35}
—	—	616 (100)	ν_{36}
570 vw	570	571 (7)	ν_{37}
544 vvw	543	544 (7)	ν_{38}
516 mw	515	519 (1)	ν_{39}
428 w	—	418 (4)	ν_{40}
346 sh, vvw	—	343 (11)	ν_{41}
330 w	—	328 (21)	ν_{42}
310 vw	—	312 (23)	ν_{43}
257 br, w	—	263 (16)	ν_{44}
241 vw	—	ca. 255 sh	ν_{45}
221 br, vw	—	228 (15)	ν_{46}
203 vw	—	204 sh	ν_{47}
203 vw	—	192 (23)	ν_{48}
185 vvw	—	—	ν_{49}
175 vvw	—	—	ν_{50}
163 vw	—	156 (13)	ν_{51}
144 vw	—	—	ν_{52}
135 vvw	—	—	ν_{53}
114 vw	—	118 br (1)	ν_{54}
95 vw	—	86 (4)	ν_{55}

^a Raman intensities in parentheses, relative to the 616 cm^{-1} band. In this scale, the intensities of the very intense bands located at 2977 and 2912 cm^{-1} are 267 and 720, respectively.

for the 57 normal modes of vibration of $\text{CF}_3\text{SO}_2\text{O-Si}(\text{CH}_3)_3$ appear in Table 4, together with the observed values. The corresponding force field in Cartesian coordinates was transformed to the set of local symmetry coordinates defined in Table 3 and the potential energy distribution was subsequently calculated (Table 4). The band wavenumbers observed in the much simpler vibrational spectra of $\text{CF}_3\text{SO}_2\text{OSiH}_3$ are also shown in Table 4 for comparison purposes. The force field in local

symmetry coordinates is available from the authors on request.

Many of the normal modes of vibration are quite near in wavenumbers and the corresponding bands could not be resolved into the individual components. The bands due to the vibrations of the methyl groups are clear examples of such a situation.

The proposed assignments of Table 4 are based on the calculated wavenumbers, infrared and Raman intensities and potential energy distribution but also

Table 3

Local symmetry coordinates for $\text{CF}_3\text{SO}_2\text{OSi}(\text{CH}_3)_3$. The definitions of internal coordinates appear in Fig. 1

Coordinate ^a	Description
$S_1 = 2p_1 - p_2 - p_3$	ν CH_3 antisymm.
$S_2 = 2p_1' - p_2' - p_3'$	
$S_3 = 2p_1'' - p_2'' - p_3''$	
$S_4 = p_2 - p_3$	
$S_5 = p_2' - p_3'$	
$S_6 = p_2'' - p_3''$	
$S_7 = p_1 + p_2 + p_3$	ν CH_3 symmetric
$S_8 = p_1' + p_2' + p_3'$	
$S_9 = p_1'' + p_2'' + p_3''$	
$S_{10} = 2\pi_1 - \pi_2 - \pi_3$	δ CH_3 antisymm.
$S_{11} = 2\pi_1' - \pi_2' - \pi_3'$	
$S_{12} = 2\pi_1'' - \pi_2'' - \pi_3''$	
$S_{13} = \pi_2 - \pi_3$	
$S_{14} = \pi_2' - \pi_3'$	
$S_{15} = \pi_2'' - \pi_3''$	
$S_{16} = r_1 - r_2$	ν SO_2 antisymm.
$S_{17} = \pi_1 + \pi_2 + \pi_3 - \varphi_1 - \varphi_2 - \varphi_3$	δ CH_3 symmetric
$S_{18} = \pi_1' + \pi_2' + \pi_3' - \varphi_1' - \varphi_2' - \varphi_3'$	
$S_{19} = \pi_1'' + \pi_2'' + \pi_3'' - \varphi_1'' - \varphi_2'' - \varphi_3''$	
$S_{20} = d_1 + d_2 + d_3$	ν CF_3 symmetric
$S_{21} = 2d_1 - d_2 - d_3$	ν CF_3 antisymm.
$S_{22} = d_2 - d_3$	
$S_{23} = r_1 + r_2$	ν SO_2 symmetric
$S_{24} = l$	ν S–O
$S_{25} = 2\varphi_1 - \varphi_2 - \varphi_3$	ρ CH_3
$S_{26} = \varphi_2 - \varphi_3$	
$S_{27} = 2\varphi_1' - \varphi_2' - \varphi_3'$	ρ CH_3
$S_{28} = \varphi_2' - \varphi_3'$	
$S_{29} = 2\varphi_1'' - \varphi_2'' - \varphi_3''$	ρ CH_3
$S_{30} = \varphi_2'' - \varphi_3''$	
$S_{31} = \epsilon_1 + \epsilon_2 + \epsilon_3 - \beta_1 - \beta_2 - \beta_3$	δ CF_3 symmetric
$S_{32} = 2q_1 - q_2 - q_3$	νSiC_3 antisymm.
$S_{33} = q_2 - q_3$	
$S_{34} = h$	ν Si–O
$S_{35} = \Psi + \Psi' - \gamma - \gamma'$	wag SO_2
$S_{36} = q_1 + q_2 + q_3$	ν SiC_3 symmetric
$S_{37} = 2\epsilon_1 - \epsilon_2 - \epsilon_3$	δ CF_3 antisymm.
$S_{38} = \epsilon_2 - \epsilon_3$	
$S_{39} = 4\phi - \Psi - \Psi' - \gamma - \gamma'$	δ SO_2
$S_{40} = \Psi - \Psi' + \gamma - \gamma'$	rock SO_2
$S_{41} = 4\theta - \Psi - \Psi' - \gamma - \gamma'$	δ CSO
$S_{42} = \lambda_1 + \lambda_2 + \lambda_3 - \mu_1 - \mu_2 - \mu_3$	δ SiC_3 symmetric
$S_{43} = t$	ν C–S
$S_{44} = 2\mu_1 - \mu_2 - \mu_3$	ρ SiC_3
$S_{45} = \mu_2 - \mu_3$	
$S_{46} = 2\lambda_1 - \lambda_2 - \lambda_3$	δ SiC_3 antisymm.

Table 3 (continued)

Coordinate ^a	Description
$S_{47} = \lambda_2 - \lambda_3$	
$S_{48} = 2\beta_1 - \beta_2 - \beta_3$	ρ CF_3
$S_{49} = \beta_2 - \beta_3$	
$S_{50} = \Psi - \Psi' - \gamma + \gamma'$	twist SO_2
$S_{51} = \tau \text{CH}_3$	torsion CH_3
$S_{52} = \tau' \text{CH}_3$	torsion CH_3
$S_{53} = \tau'' \text{CH}_3$	torsion CH_3
$S_{54} = \alpha$	δ SOSi
$S_{55} = \tau \text{S–O}$	torsion S–O
$S_{56} = \tau \text{CF}_3$	torsion CF_3
$S_{57} = \tau \text{SiC}_3$	torsion SiC_3

^a Redundant coordinates were taken in a first approximation as the sum of the angles around C2, S5, Si8, C9, C13 and C17.

on the comparison with the reported data for the related molecules $\text{CF}_3\text{SO}_2\text{OSiH}_3$ [1], $(\text{CH}_3)_3\text{SiOCH}_3$ and $(\text{CH}_3)_3\text{SiOCH}=\text{CH}_2$ [9]. The assignments for some bands are commented on in what follows.

Only two bands located at 2970 and 2915 cm^{-1} (gas) are observed for the nine CH_3 stretching modes (Figs. 3 and 5), which correspond to the anti-symmetric and the symmetric stretchings, respectively, according with their relative infrared and Raman intensities. Such results agree with the ordering predicted by the calculation and observed in related molecules having the $\text{Si}(\text{CH}_3)_3$ grouping [9].

The deformation modes of the three CH_3 groups give rise to bands in the 1443–1411 cm^{-1} region (antisymmetric deformations) and the 1264–1249 cm^{-1} region (symmetric deformations) in $(\text{CH}_3)_3\text{SiOCH}_3$ and $(\text{CH}_3)_3\text{SiOCH}=\text{CH}_2$ [9]. Therefore, the 1420 and 1249 cm^{-1} Raman bands are assigned to these modes. The last band appears clearly split in two components in the infrared spectra, although a third band due to the CF_3 symmetric stretch should be also contributing to this complex feature.

The six rocking vibrations of the CH_3 groups appear at 865–842 and 769–754 cm^{-1} in the above-mentioned compounds [9]. The corresponding bands in $\text{CF}_3\text{SO}_2\text{OSi}(\text{CH}_3)_3$ should be those located at 857 cm^{-1} (showing a shoulder in the low wavenumbers flange) and 767 cm^{-1} in the gas. In accordance with the potential energy distribution, these bands are assigned to the perpendicular and parallel CH_3 rockings, respectively, being that assignment reversed in comparison with the cited reference. A mode

Table 4
Observed and calculated wavenumbers for $\text{CF}_3\text{SO}_2\text{OSi}(\text{CH}_3)_3$, potential energy distribution and comparison with data for $\text{CF}_3\text{SO}_2\text{OSiH}_3$ (ν , stretching; δ , deformation; ρ , rocking; τ , torsion; rock, rocking; wag, wagging; tw, twisting; s, symmetric; a, antisymmetric)

Mode	Observed	Calculated		Infrared int. ^b	Raman int. ^c	P.E.D. (contributions $\geq 10\%$)		Assignments	Observed $\text{CF}_3\text{SO}_2\text{OSiH}_3^a$
		Wavenumber	Wavenumber						
1	2970	3145	2.93	74.0		$28\text{S}_3 + 16\text{S}_4 + 141\text{S}_6$		$\nu \text{CH}_3 \text{ a}$	
2		3141	3.02	54.1		91S_5			
3		3135	6.15	78.2		97S_4			
4		3126	17.4	152.		$19\text{S}_1 + 61\text{S}_3 + 13\text{S}_4$			
5		3124	4.64	28.6		$58\text{S}_1 + 15\text{S}_2 + 20\text{S}_3 + 11\text{S}_4$			
6		3122	1.52	52.1		$22\text{S}_1 + 71\text{S}_2$			
7	2915	3050	3.39	200.		$18\text{S}_3 + 11\text{S}_4 + 107\text{S}_9$		$\nu \text{CH}_3 \text{ s}$	
8		3047	1.51	99.6		$49\text{S}_7 + 33\text{S}_8 + 21\text{S}_9$			
9		3046	0.74	30.9		$42\text{S}_7 + 57\text{S}_8$			
10	1420	1491	11.5	1.62		$20\text{S}_{10} + 36\text{S}_{11} + 34\text{S}_{12}$		$\delta \text{CH}_3 \text{ a}$	
11		1478	1.78	0.96		$24\text{S}_{11} + 21\text{S}_{12} + 24\text{S}_{13} + 21\text{S}_{15}$			
12		1475	1.92	13.1		$55\text{S}_{14} + 33\text{S}_{15}$			
13		1470	0.150	36.3		$59\text{S}_{10} + 23\text{S}_{11}$			
14		1469	0.505	23.4		$13\text{S}_{10} + 32\text{S}_{12} + 39\text{S}_{13}$			
15		1460	0.117	0.92		$26\text{S}_{13} + 34\text{S}_{14} + 35\text{S}_{15}$			
16	1414	1365	242.	1.59		95S_{16}		$\nu \text{SO}_2 \text{ a}$	1405
17	1264–1255	1327	30.	0.57		$39\text{S}_{17} + 32\text{S}_{18} + 28\text{S}_{19}$		$\delta \text{CH}_3 \text{ s}$	
18		1318	45.7	0.66		$60\text{S}_{17} + 34\text{S}_{18}$			
19		1317	46.3	0.77		$34\text{S}_{18} + 65\text{S}_{19}$			
20		1221	55.3	3.42		$34\text{S}_{20} + 26\text{S}_{23} + 25\text{S}_{30} + 20\text{S}_{43}$		$\nu \text{CF}_3 \text{ s} + \nu \text{SO}_2 \text{ s} + \delta \text{CF}_3 \text{ s}$	1250
21	1221	1268	240.	0.78		$72\text{S}_{21} + 26\text{S}_{22} + 11\text{S}_{37}$		$\nu \text{CF}_3 \text{ a}$	1212
22		1252	232.	2.76		$25\text{S}_{21} + 68\text{S}_{22} + 12\text{S}_{38}$			1212
23	1163	1127	233.	4.74		$22\text{S}_{20} + 64\text{S}_{23} + 13\text{S}_{31}$		$\nu \text{SO}_2 \text{ s}$	1152
24		962	82.7	6.28		$32\text{S}_{24} + 12\text{S}_{25} + 11\text{S}_{27} + 10\text{S}_{29}$		$\nu \text{S-O}$	887
25	857	899	125.	1.38		$25\text{S}_{28} + 33\text{S}_{30} + 12\text{S}_{32}$		ρCH_3	
26		895	108.	1.13		$40\text{S}_{26} + 13\text{S}_{28} + 12\text{S}_{33}$			
27	842	869	665.	1.30		$41\text{S}_{24} + 12\text{S}_{29} + 32\text{S}_{34}$		$\nu \text{S-O} + \nu \text{Si-O}$	
28	767	790	23.7	6.80		$28\text{S}_{25} + 34\text{S}_{27} + 12\text{S}_{32}$		ρCH_3	
29		788	20.4	2.54		$15\text{S}_{25} + 41\text{S}_{29} + 14\text{S}_{33}$			
30		765	10.8	2.13		$37\text{S}_{20} + 28\text{S}_{31} + 17\text{S}_{43}$		$\nu \text{CF}_3 \text{ s} + \delta \text{CF}_3 \text{ s}$	774
31	705	709	0.703	0.02		$37\text{S}_{26} + 36\text{S}_{28} + 43\text{S}_{30}$		ρCH_3	
32		707	6.86	6.08		$19\text{S}_{25} + 60\text{S}_{32}$		$\nu \text{SiC}_3 \text{ a}$	
33		701	3.63	5.16		$12\text{S}_{27} + 18\text{S}_{29} + 60\text{S}_{33}$			
34	683	673	15.2	1.14		$10\text{S}_{24} + 34\text{S}_{34} + 11\text{S}_{35} + 22\text{S}_{36}$		$\nu \text{Si-O} + \nu \text{SiC}_3 \text{ s}$	678
35	630	602	130.	0.93		$20\text{S}_{31} + 38\text{S}_{35} + 10\text{S}_{36} + 12\text{S}_{39}$		$\text{Wag SO}_2 + \delta \text{CF}_3 \text{ s}$	
36	616	597	12.4	19.6		61S_{36}		$\nu \text{SiC}_3 \text{ s}$	
37	570	557	4.37	2.21		$13\text{S}_{37} + 32\text{S}_{38} + 12\text{S}_{40}$		$\delta \text{CF}_3 \text{ a}$	566
38	544	536	5.07	2.83		$39\text{S}_{37} + 23\text{S}_{38}$			550

Table 4 (continued)

Mode	Observed	Calculated		Infrared int. ^b	Raman int. ^c	P.E.D. (contributions $\geq 10\%$)	Assignments	Observed $\text{CF}_3\text{SO}_2\text{OSiH}_3^a$
		Wavenumber						
39	516	495	22.0	0.30	19S ₃₇ + 38S ₃₉	δSO_2		500
40	428	402	17.3	2.11	18S ₃₄ + 13S ₃₈ + 20S ₃₉ + 27S ₄₀	rock SO_2 + δSO_2		428
41	343	328	1.89	1.43	16S ₃₉ + 27S ₄₁ + 14S ₄₅ + 14S ₄₈ + 17S ₄₉ + 18S ₅₀	δCSO + tw SO_2 + ρCF_3		318 (calc.)
42	330	313	4.86	1.91	13S ₄₃ + 20S ₄₈ + 10S ₅₀	ρCF_3		328
43	310	300	6.78	2.54	14S ₄₂ + 32S ₄₃ + 14S ₄₅	νCS		299
44	257	251	6.65	0.97	11S ₃₅ + 34S ₄₅ + 22S ₄₇ + 22S ₄₈	ρSiC_3		
45	241	239	4.68	0.80	13S ₂₈ + 25S ₄₄ + 53S ₄₆	$\delta \text{SiC}_3 \text{ a}$		
46	221	214	5.18	0.48	58S ₄₂ + 14S ₄₆ + 18S ₄₇ + 14S ₄₈	$\delta \text{SiC}_3 \text{ s}$		
47	203	196	0.471	0.09	11S ₄₁ + 19S ₄₂ + 18S ₄₅ + 61S ₄₇	$\delta \text{SiC}_3 \text{ a}$		
48	192	189	2.02	0.97	34S ₄₀ + 55S ₄₉ + 45S ₅₀	ρCF_3 + tw SO_2		204
49	185	175	0.545	0.76	13S ₂₅ + 65S ₄₄ + 49S ₄₆	ρSiC_3 + $\delta \text{SiC}_3 \text{ a}$		
50	175	159	0.105	0.14	71S ₅₂ + 27S ₅₃	τCH_3		
51	163	151	0.532	0.19	12S ₄₁ + 11S ₄₅ + 13S ₄₇ + 16S ₅₂ + 43S ₅₃	τCH_3		
52	144	135	1.26	0.36	39S ₄₁ + 19S ₄₅ + 12S ₄₈ + 22S ₅₁ + 16S ₅₃	δCSO		
53	135	127	0.003	0.10	72S ₅₁ + 18S ₅₂ + 23S ₅₃	τCH_3		
54	114	106	0.996	0.23	11S ₄₄ + 73S ₅₄	δSOSi		138 (calc.)
55	95	52	0.448	0.01	102S ₅₅ + 43S ₅₇	τSO_2		
56	–	41	0.405	0.01	86 S ₅₆	τCF_3		39 (calc.)
57	–	24	0.154	0.00	18S ₄₅ + 40S ₅₅ + 20S ₅₆ + 79S ₅₇	τSiC_3		

^a Data from Ref. [1].^b Infrared intensities in km mol^{-1} .^c Raman activities from the HF/6-31G** calculation; units are $\text{\AA}^4 (\text{amu})^{-1}$.

comprising perpendicular CH_3 rockings, predicted at 709 cm^{-1} and very weak in infrared, should be contributing to the 705 cm^{-1} band. In fact, according with the calculations this last, relatively weak band, should result from the overlapping of three components (see Table 4).

The two remaining components of the 705 cm^{-1} band should be the SiC_3 antisymmetric stretching modes. The symmetric stretching mode of that group appears as a very intense Raman band at 616 cm^{-1} , as happens also with $(\text{CH}_3)_3\text{SiOCH}_3$ at 601 cm^{-1} and $(\text{CH}_3)_3\text{SiOCH}=\text{CH}_2$ at 615 cm^{-1} [9]. The deformation and rocking modes of the SiC_3 group appear strongly coupled with vibrations of the rest of the molecule, as shown by the calculations. The symmetric SiC_3 deformation is predicted at 214 cm^{-1} , near the Raman band at 228 cm^{-1} , which is therefore assigned to that mode; this assignment agrees with the $208\text{--}211\text{ cm}^{-1}$ values reported for the above-mentioned molecules [9]. The very weak infrared band located at 241 cm^{-1} , with a shoulder at 255 cm^{-1} in Raman as counterpart, is assigned to one of the SiC_3 antisymmetric deformations. Such a mode was observed as a very weak infrared band at 245 cm^{-1} in $(\text{CH}_3)_3\text{SiOCH}_3$ [9].

The 1414 and 1163 cm^{-1} bands are assigned immediately to the antisymmetric and the symmetric $\text{O}=\text{S}=\text{O}$ stretchings, respectively. Such modes appear at 1405 and 1152 cm^{-1} in $\text{CF}_3\text{SO}_2\text{OSiH}_3$ [1].

Between the two bands mentioned last appear the features located at 1254 and 1221 cm^{-1} . The first one, which appears as a doublet in the infrared spectra, results from the overlapping of bands due to the symmetric CF_3 stretching and the symmetric CH_3 deformations, as mentioned before. The 1221 cm^{-1} band, broad in the infrared spectrum of the liquid, should result from the two quasi-degenerated CF_3 antisymmetric stretchings. Here again, the experiment suggests an ordering for the CF_3 stretchings which is the reverse of that predicted by the calculation (Table 4), as was observed before for $\text{CF}_3\text{SO}_2\text{OSiH}_3$ and other related molecules having the CF_3SO_2 moiety [1]. The symmetric CF_3 deformation band, usually weak in this type of compound, is probably overlapped by the band located at 767 cm^{-1} , of medium intensity. The bands located at 570 and 544 cm^{-1} are immediately assigned to the non-degenerate antisymmetric CF_3 deformation modes.

Only one of the three modes associated with the CH_3 torsions has a predicted appreciable intensity in infrared, with a wavenumber equal to 151 cm^{-1} . A very weak band at 163 cm^{-1} in the FIR spectrum is assigned to such a mode, having its Raman counterpart at 156 cm^{-1} .

The CSO and SOSi skeletal deformations should originate the weak infrared features located at 144 and 114 cm^{-1} , respectively. The first mentioned vibration contributes also appreciably to ν_{41} , ν_{47} and ν_{51} , according to the potential energy distribution (Table 4).

The CF_3 torsional mode, not observed, is predicted at a considerably low wavenumber, 41 cm^{-1} , comparable with the value of 39 cm^{-1} calculated for $\text{CF}_3\text{SO}_2\text{OSiH}_3$ [1]. A weak Raman feature at 95 cm^{-1} could be the torsional mode associated with the S5-O7 bond, predicted at 52 cm^{-1} but probably shifted to a higher value in the liquid substance, although such an assignment is only speculative. Finally, the SiC_3 torsional mode is predicted at 24 cm^{-1} , but not observed in our spectra.

5. Conclusions

An optimized molecular geometry was determined for $\text{CF}_3\text{SO}_2\text{OSi}(\text{CH}_3)_3$ using the B3LYP/6-31G** quantum chemistry method. A scan of the potential energy surface showed that the optimized conformation, with the $\text{Si}(\text{CH}_3)_3$ group in a *gauche* position with respect to the rest of the molecule, correspond to one of two symmetrically located minima separated by a very low barrier. The infrared and Raman spectra of the substance were also obtained and an assignment of the observed features was proposed on the basis of comparison with related molecules and with wavenumbers, infrared and Raman intensities and potential energy distribution calculated also with quantum chemistry procedures.

Acknowledgements

The research grants of CONICET, ANPCYT, CIC-PBA and UNLP are gratefully acknowledged, as well as the financial help received from CIUNT.

References

- [1] L.E. Fernández, A. Ben Altabef, A. Navarro, M.F. Gómez, E.L. Varetti, *Spectrochim. Acta* 56A (2000) 1101.
- [2] A.D. Becke, *J. Chem. Phys.* 98 (1993) 5648.
- [3] C. Lee, W. Yang, R.G. Parr, *Phys. Rev. B* 37 (1988) 785.
- [4] M.J. Frisch, G.W. Trucks, H.B. Schlegel, P.M.W. Gill, B.G. Johnson, M.A. Robb, J.R. Cheeseman, T. Keith, G.A. Petersson, J.A. Montgomery, K. Raghavachari, M.A. Al-Laham, V.G. Zakrzewski, J.B. Ortiz, J.B. Foresman, J. Cioslowski, B.B. Stefanov, A. Nanayakkara, M. Challacombe, C.Y. Peng, P.Y. Ayala, W. Chen, M.W. Wong, J.L. Andres, E.S. Replogle, R. Gomperts, R.L. Martin, D.J. Fox, J.S. Binkley, D.J. Defrees, J. Baker, J.P. Stewart, M. Head-Gordon, C. Gonzalez, J.A. Pople, *GAUSSIAN94*, Revision D.3, Gaussian Inc., Pittsburgh, PA, 1995.
- [5] E.B. Wilson, J.D. Decius, P.C. Cross, *Molecular Vibrations*, McGraw-Hill, New York, 1955.
- [6] W.B. Collier, Program FCARTP (QCPE #631), Department of Chemistry, Oral Roberts University, Tulsa, OK, 1992.
- [7] Program HYPERCHEM, Hypercube Inc., 1993.
- [8] F. Trautner, A. Ben Altabef, L.E. Fernández, E.L. Varetti, H. Oberhammer, *Inorg. Chem.* 38 (1999) 3051.
- [9] J. Dedier, A. Marchand, M.T. Forel, E. Frainnet, *J. Organomet. Chem.* 81 (1974) 161.